

Bounds on the $g_{KN\Sigma}^2$ coupling constant from positivity and charge-exchange data

J. Antolin

Departamento de Física Teórica, Facultad de Ciencias, Universidad de Zaragoza, 50009 Zaragoza, Spain

(Received 25 June 1986)

Positivity of the imaginary part of the forward K^-n elastic amplitude on the unphysical cut allows the calculation of bounds on the $g_{KN\Sigma}^2$ coupling constant using the forward differential cross sections of the charge-exchange reaction $K^-p \rightarrow \bar{K}^0n$, the scarce K^-n real-part data, and a Stieltjes parametrization of the K^-p real-part data. The bounds on the coupling constant are $2.11 < g_{KN\Sigma}^2 < 3.70$ and real parts of the $K^\pm n$ amplitudes are also obtained, as well as the position of the complex-conjugate zeros of the K^-n amplitude: $(0.35 \pm 0.05) \pm (0.16 \pm 0.04)i$ GeV/c.

I. INTRODUCTION

The analysis of the $K^\pm n$ amplitude has received much less attention than the $K^\pm p$ amplitude owing to the lack of $K^\pm n$ real-part data and also to their inaccuracy related to the deuteron structure. For many years it has been normal to deal with the abundant $K^\pm p$ data and calculate the value of the effective KNY coupling constant $G^2 = g_{KN\Lambda}^2 + 0.9g_{KN\Sigma}^2$ (Ref. 1). As a consequence the knowledge of the $K^\pm p$ amplitude has improved significantly during the last few years in such a way that it is possible to tabulate real and imaginary parts of this amplitude.

Both model-independent methods² and K -matrix parametrizations³ agree basically in the determination of the real and imaginary parts of the $K^\pm p$ amplitude. On the other hand, there are a few papers trying to analyze, using model-dependent methods,^{4,5} the $K^\pm n$ amplitude, and there is no model-independent method directly applied to this amplitude.

In spite of the instability associated to the analytic extrapolation starting from functional data affected by errors caused by experimental measurements, there are nowadays powerful methods to stabilize this sort of extrapolation.⁶ The basic ingredients are some general properties of the functions (besides analyticity), which limit the universe of admissible parametrizations fitting the data in such a way that small perturbations in the data region do not give rise to very different predictions outside the experimental region.

We have recently used positivity to produce a stable method for analytic extrapolation, not only when the experimental errors tend to zero, but when one uses the true experimental errors, which are often larger than one could wish.⁷

We use in this paper, as an hypothesis, the positivity of the imaginary part of the K^-n amplitude on the unphysical cut without using any concrete parametrization. This general property allows the use of the rigorous properties of Padé approximants (PA) to Stieltjes functions and provides also rigorous bounds on the coupling constant.

The unphysical region also receives a contribution from the $Y_1^*(1385)$ resonance which occurs in the $I=1$ $P_{3/2}$ state of the $\bar{K}N$ system and, being in a P wave, gives a negative contribution to the imaginary part of the unphys-

ical cut. We assume that the nonresonant S wave is dominant on the unphysical cut so we have our positivity hypothesis.

It is difficult to get model-independent reliable results by using only the five $K^\pm n$ real-part data⁸ so we are going to use the forward differential cross sections of the charge-exchange amplitude to complement these data.

In Sec. II we transform the K^-n discrepancy function into a Stieltjes function $H_1(z)$, we obtain the coefficients of the formal series expansion of $H_1(z)$ by means of the Gronwall transformation, we recall the constraints imposed on them by positivity and how the PA built with such coefficients bound the values of $g_{KN\Sigma}^2 = g_{K^-p\Sigma^0}^2 = \frac{1}{2}g_{K^-n\Sigma^-}^2$.

In Sec. III the results on the coupling constant and real parts are presented and discussed.

II. A STIELTJES ANALYSIS OF THE K^-n AMPLITUDE

Isospin invariance gives information on the K^-n real parts through the expression

$$4 \frac{d\sigma}{4\Omega} \Big|_{\theta=0^\circ}^{\text{lab}} (K^-p \rightarrow \bar{K}^0n) = |A_p^- - A_n^-|^2 + |D_p^- - D_n^-|^2, \quad (2.1)$$

where $A_{p,n}^-$ are, respectively, the laboratory imaginary parts of the K^-p and K^-n amplitudes and $D_{p,n}^-$ their respective real parts. Thus the use of charge-exchange data can be transformed, except for the sign, into real-part K^-n data if we use the relatively well-known D_p^- real parts⁹ and the K^-p, K^-n total cross sections¹⁰ (see Fig. 1). We are going to use for D_p^- one of our parametrizations calculated in Ref. 11 by using positivity and unimodality of the imaginary part of the K^-p amplitude on the unphysical cut.

We define the discrepancy function

$$\Delta_-(\omega) \equiv \frac{1}{\pi} \int_{\omega_{\Lambda\pi}}^{\omega_u} \frac{\text{Im}F_-(\omega')d\omega'}{(\omega' - \omega)(\omega' - \omega_0)} + \frac{X_\Sigma}{(\omega_\Sigma - \omega)(\omega_\Sigma - \omega_0)}, \quad (2.2)$$

where $F_\pm(\omega)$ is the $K^\pm n$ forward elastic amplitude, ω is

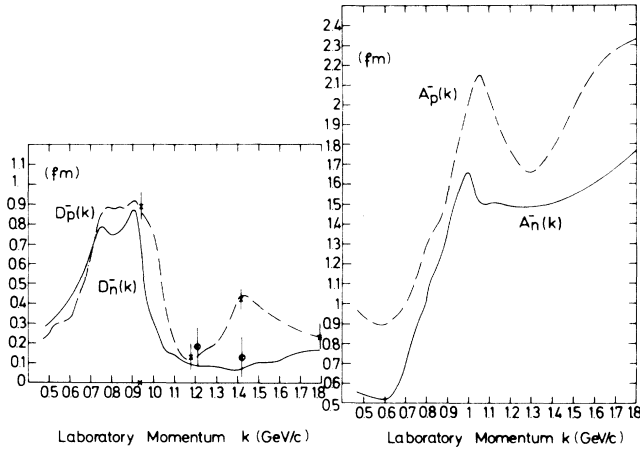


FIG. 1. The right-hand figure shows the imaginary parts of the K^-p and K^-n amplitudes, A_p^- and A_n^- (fm). The left-hand figure shows the real part of the K^-p amplitude used in this work (discontinuous line) and the result obtained for the real part of the K^-n amplitude, D_n^- (continuous line). Points marked with \times and \bullet are, respectively, the experimental D_p^- and D_n^- Coulomb-interference real parts.

the laboratory energy of the incoming kaon, ω_0 is the subtraction point, $\omega_u = 0.67$ GeV/c, $X_\Sigma = 2g_{KN\Sigma}^2[(m_\Sigma - m_n)^2 - m_K^2]/4m_n^2$, and the once-subtracted dispersion relation for the K^-n amplitude (at $\omega_0 = -m_K$) is written as

$$\Delta_-(\omega) = \frac{\text{Re}F_-(\omega) - \text{Re}F_-(\omega_0)}{\omega - \omega_0} + \frac{P}{4\pi^2} \int_{m_K}^{\infty} \frac{k'\sigma_+(\omega')d\omega'}{(\omega' + \omega)(\omega' + \omega_0)} - \frac{P}{4\pi^2} \int_{\omega_u}^{\infty} \frac{k'\sigma_-(\omega')d\omega'}{(\omega' - \omega)(\omega' - \omega_0)}, \quad (2.3)$$

where the optical theorem $\text{Im}F_{\pm}(\omega) = k\sigma_{\pm}(\omega)/4\pi$ has been used, k being the laboratory momentum of the kaon, and $\sigma_{\pm}(\omega)$ the total $K^{\pm}n$ cross sections.

In principle the discrepancy function $\Delta_-(\omega)$ could only be calculated with errors in the five points, where $\text{Re}F_{\pm}(\omega)$ has been measured [four points in the K^-n region and one in the K^+n region using $F_+(\omega) = F_-(-\omega)$] (Refs. 5 and 12) by using the relatively well-known value of $\text{Re}F_+(\omega = m_K) = -0.23$ fm from low-energy analy-

ses,^{13,14} a fit to the experimental cross sections,⁹ and a Regge parametrization for the asymptotic region.¹⁵

We use (2.1) to calculate $|D_p^- - D_n^-|$ at 115 points, where $d\sigma/d\Omega|_{\theta=0}$ (or the Legendre coefficients A_l of its expansion) has been calculated in the region between 0.475 and 1.843 GeV/c laboratory momentum of the kaon. Data are from references quoted in Table I and Fig. 2. We shall discuss later the sign determination of $D_p^- - D_n^-$ in order to have D_n^- determined in these 115 new points. Thus we shall use 120 values of D_n^- with their errors.

Using now the expressions

$$x(\omega') = \frac{\omega' - \omega_u}{\omega_{\Lambda\pi} - \omega_u}, \quad z(\omega) = \frac{\omega_u - \omega_{\Lambda\pi}}{\omega - \omega_u} \quad (2.4)$$

we can also evaluate the function

$$H_0(z) \equiv -\frac{\Delta_-(z)}{z} = \phi(z) + \frac{A}{z + z_\Sigma}, \quad (2.5)$$

where

$$\phi(z) = \int_0^1 \frac{\chi(x)dx}{1+xz}, \quad \chi(x) = \frac{\text{Im}F_-(\omega'(x))}{\pi[\omega'(x) + m_K]} \geq 0,$$

is a Stieltjes function owing to our positivity hypothesis in the unphysical region and $A = -0.303g_{KN\Sigma}^2$ (GeV/c)⁻² is the residue associated to the pole in the z plane at $z = -z_\Sigma = -0.859$.

The analytic structure of the H_0 function is the sum of a Stieltjes function with its cut in $]-\infty, -1]$, plus a pole term. The function

$$H_1(z) = \frac{H_0(z)(z + z_\Sigma) - H_0(z_1)(z_1 + z_\Sigma)}{z - z_1}, \quad (2.6)$$

where z_1 is one of the points and where we also know $H_0(z)$ is a Stieltjes function

$$H_1(z) = \int_0^1 \frac{\chi_1(x)dx}{1+xz}, \quad (2.7)$$

$$\chi_1(x) = \chi(x) \frac{1 - z_\Sigma x}{1 + z_1 x} \geq 0, \quad x \in [0, 1].$$

The Gronwall transformation^{7,23} allows one to calculate the first coefficients of the series expansion of $H_1(z)$:

$$H_1(z) = \sum_{n=0}^{\infty} h_n(-z)^n, \quad h_n = \int_0^1 \chi_1(x)x^n dx \quad (2.8)$$

using exclusively experimental data.

TABLE I. Experimental data on $d\sigma/d\Omega|_{\theta=0}$ used in this work.

Authors	Ref.	Number of points	$P_{\text{lab}} = k$ range (GeV/c)
R. Armenteros <i>et al.</i> (1970)	16	17	0.475–0.80
M. Alston-Garnjost <i>et al.</i> (1978)	17	23	0.515–0.956
A. J. Van Horn <i>et al.</i> (1972)	18	19	0.800–1.520
M. Jones <i>et al.</i> (1975)	19	9	0.862–1.001
R. J. Hemingway <i>et al.</i> (1975)	20	23	1.136–1.798
B. Conforto <i>et al.</i> (1976)	21	11	0.960–1.355
P. J. Litchfield <i>et al.</i> (1971)	22	13	1.263–1.843

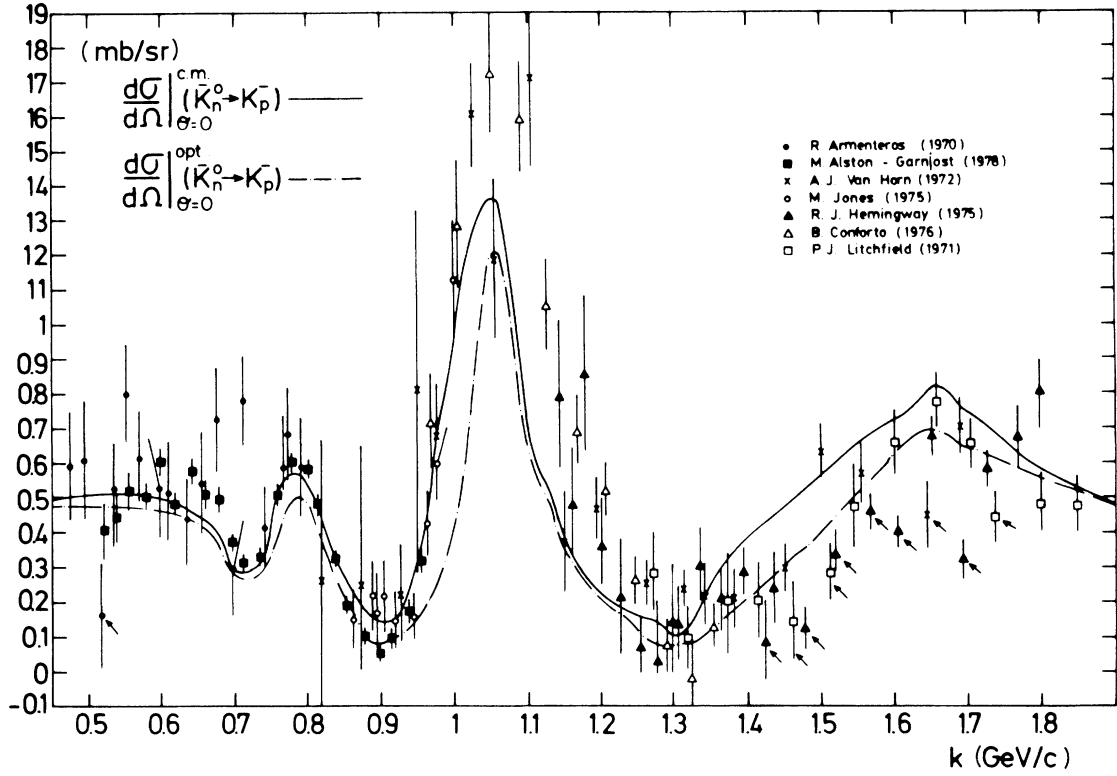


FIG. 2. Experimental data on $d\sigma/d\Omega|_{\theta=0}$ used in the fits. The points are from Refs. 16–22. Points marked with an arrow are the points violating the optical limit (discontinuous line). The continuous line is the result of this work.

TABLE II. Bounds on the $g_{KN\Sigma^2}$ coupling constant from charge-exchange data. Column 1 contains the absorption case. Columns 2 and 3 contain the position of the absorption point in the k and z planes, respectively, column 4 the number of points considered in the fit without (above) and with (below) positivity. Columns 5, 6, and 7 contain the values of the coefficients h_0 and h_1 and relative χ^2 of the fit. Columns 8 and 9 contain the lower and upper bounds calculated with the error bars in h_0 and h_1 (above) and central values (below).

Case	Absorption point		Number of points	$h_0 \pm h_0^e$	$h_1 \pm h_1^e$	χ_R^2	Bounds on $g_{KN\Sigma^2}$	
	k	z_1					Lower	Upper
a	0.515	9.638	108	0.121 ± 0.016	-0.019 ± 0.008	538.4/108-2	-0.92	29.07
			76	0.141 ± 0.018	0.017 ± 0.010	71.2/76-2	-0.36	25.15
b	0.536	7.110	108	0.151 ± 0.017	-0.008 ± 0.010	586.6/108-2	0.76	5.78
			77	0.167 ± 0.019	0.024 ± 0.012	65.5/77-2	1.09	3.70
c	0.556	5.707	108	0.171 ± 0.019	-0.009 ± 0.011	569.0/108-2	-0.09	27.79
			76	0.183 ± 0.021	0.026 ± 0.013	61.2/76-2	0.64	24.65
d	0.577	4.766	108	0.191 ± 0.020	0.012 ± 0.014	568.3/108-2	1.68	4.36
			75	0.172 ± 0.023	0.031 ± 0.016	59.7/75-2	0.66	26.76
							1.28	23.82
							1.49	7.16
							2.11	4.98
							1.41	26.00
							1.79	23.40
							1.25	7.09
							2.01	4.91

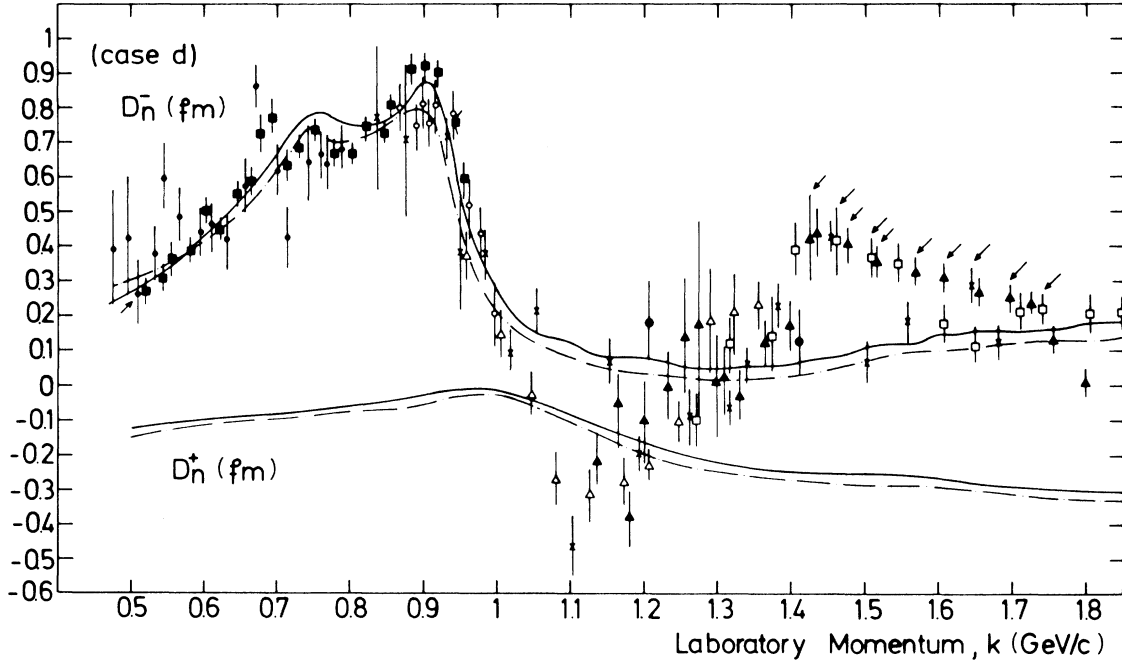


FIG. 3. Corridor for the real parts of the $K^\pm n$ amplitude and “experimental real-part data” used in the fits of Table II. The discontinuous and continuous lines correspond, respectively, to the PA and complementary PA.

The positivity conditions for the function $\chi_1(x)$ in the unit interval do not allow the h_n coefficients to be arbitrary, but rather the moments of a positive function, so we have the Hankel constraints^{7,24}

$$H_n^m(\Delta^k) = \begin{vmatrix} \Delta_m^k & \Delta_{m+1}^k & \cdots & \Delta_{m+n}^k \\ \Delta_{m+1}^k & \Delta_{m+2}^k & \cdots & \Delta_{m+n+1}^k \\ \vdots & \vdots & \ddots & \vdots \\ \Delta_{m+n}^k & \Delta_{m+n+1}^k & \cdots & \Delta_{m+2n}^k \end{vmatrix} > 0, \quad (2.9)$$

where $\Delta_p^0 = h_p$, $\Delta_p^k = \Delta_p^{k-1} - \Delta_{p+1}^{k-1}$, $p = 0, 1, \dots$; $k = 1, 2, \dots$.

The conditions for the first coefficients are

$$h_0 > 0, \quad h_0 > h_1 > 0, \quad h_1 > h_2 > \frac{(h_1)^2}{h_0} > 0. \quad (2.10)$$

Using now rigorous bounding properties of PA to Stieltjes functions and undoing the transformation (2.6) with the approximants instead of the function, we obtain the approximants to $H_0(z)$. All these approximants to $H_0(z)$ have a pole, as $H_0(z)$ itself, at $z = -z_\Sigma$ providing bounds on the $g_{KN\Sigma}^2$ coupling constant. As the bounding properties of PA on Stieltjes functions are valid on the whole complex plane except the Stieltjes cut $]-\infty, -1]$, which is the transformation of the unphysical cut in the ω plane $[\omega_{\Lambda\pi}, \omega_u]$, we also have, using (2.3), the values of the real parts of the amplitude for real ω (including the unphysical point $\omega=0$). The validity of the PA for complex ω allows one to calculate also the complex-conjugated zeros of the amplitude. As can be seen the “physical” region for PA is much larger than the physical

region of the $K^\pm n$ amplitude; therefore, poles and zeros of the amplitude are treated in a completely similar manner as values of the amplitude at physical energies.

III. RESULTS

We have chosen as absorption points z_1 the four points of lowest momentum of the $K^- n$ cut, where the differential cross sections at $\theta=0$ of the charge-exchange reaction have been recently measured with great accuracy (cases a, b, c, d) (Ref. 17). The reason for this choice has been that these points are transformed into the z plane in a sufficiently remote region ($z = 4.77-9.64$) to avoid the instabilities associated with the absorption process, (2.6), when the absorption is performed in a region where experimental points are too close to the absorption point.

Figure 2 shows the optical contribution $d\sigma/d\Omega|_{\theta=0}^{\text{opt}}$ (taking into account only imaginary parts) to $d\sigma/d\Omega|_{\theta=0}(K^- p \rightarrow \bar{K}^0 n)$.

The analysis of the data is based on three facts: (i) The violation (or saturation) of the optical contribution by some of the experimental points of the differential cross section of the reaction $K^- p \rightarrow \bar{K}^0 n$; (ii) the selection of the sign of $D_p^- - D_n^-$; (iii) the constraints (2.9) the first coefficients of the series expansion of $H_1(z)$ must satisfy.

With regard to condition (i) we performed calculations both with and without those points, assuming in the first case that $D_p^- = D_n^-$ for such a point.

Fits with all experimental points did not satisfy the positivity conditions for the two first coefficients h_0, h_1 , and we discarded 11 points which, with their error bars, were below $d\sigma/d\Omega|_{\theta=0}^{\text{opt}}$ and kept points whose error bars touched at least the optical limit, assuming once more

TABLE III. Corridor for the real parts of the $K^\pm n$ amplitude obtained with positivity.

k	D_n^- (fm)		D_n^+ (fm)	
0.50	0.28	0.31	-0.12	-0.14
0.55	0.32	0.34	-0.11	-0.13
0.60	0.42	0.41	-0.09	-0.11
0.65	0.54	0.51	-0.09	-0.10
0.70	0.67	0.62	-0.08	-0.09
0.75	0.78	0.74	-0.07	-0.08
0.80	0.75	0.70	-0.06	-0.08
0.85	0.76	0.74	-0.04	-0.06
0.90	0.87	0.80	-0.02	-0.05
0.95	0.54	0.47	-0.02	-0.04
1.00	0.26	0.20	-0.01	-0.03
1.10	0.13	0.09	-0.08	-0.11
1.20	0.09	0.05	-0.16	-0.20
1.21	0.09	0.05	-0.16	-0.20
1.30	0.05	0.02	-0.22	-0.25
1.40	0.07	0.03	-0.24	-0.27
1.42	0.08	0.04	-0.24	-0.27
1.50	0.12	0.07	-0.25	-0.29
1.60	0.15	0.10	-0.26	-0.29
1.70	0.16	0.12	-0.28	-0.31
1.80	0.18	0.13	-0.29	-0.33
1.90	0.21	0.15	-0.31	-0.35
2.00	0.20	0.15	-0.33	-0.36
2.50	0.24	0.17	-0.36	-0.43
2.61	0.25	0.18	-0.37	-0.44
3.00	0.28	0.21	-0.41	-0.48
4.00	0.33	0.28	-0.46	-0.54
5.00	0.35	0.32	-0.51	-0.57
10.00	0.46	0.40	-0.47	-0.53
20.00	0.75	0.63	-0.44	-0.51
40.00	1.21	1.05	-0.12	-0.16
60.00	1.67	1.52	-0.02	-0.09
80.00	2.29	2.12	+ 0.70	+ 0.61
100.00	3.02	2.75	+ 1.11	+ 0.89

$D_p^- = D_n^-$ for such points and an uncertainty equal to the experimental one.

As for condition (ii), we performed fits taking into account the different possibilities of the sign of $D_p^- - D_n^-$ in different regions of the experimental range. All fits violate positivity conditions for the coefficients h_0 and h_1 except those ones in which $D_p^- < D_n^-$ in the 0.5–0.7 GeV/c region and $D_p^- > D_n^-$ in the rest of the experimental region. The coefficients for these fits with the 108 points²⁵ satisfy $h_0 > 0$ but not the condition $h_1 > 0$ in general (see Table II). The bounds so obtained, with this number of experimental points, and therefore without positivity, are also quoted in Table II as well as the poor-ness of the fits.

As every Stieltjes function passing through the point

$(0, h_0)$ is rigorously bounded on the real axis, except on the cut, by the PA, $[0/0] = h_0$ and $[0/0]^c = h_0/(1+z)$, we have taken into account the corridor determined by $h_0 \pm 2h_0^e$ as in Ref. 11 to filtrate our 108 points.

The experimental points which, with their error bars, lie outside the allowed corridor have been rejected. The results of the fits with the filtered experimental set are in Table II. The discarded points are basically independent of the absorption point chosen.

The bounds for $g_{KN\Sigma^2}$ obtained with these values of $h_0 \pm h_0^e$ and $h_1 \pm h_1^e$ and the positivity bounds for h_2 , (2.11), are also in Table II, the common allowed region for the four cases being

$$1.49 < g_{KN\Sigma^2} < 5.78 \quad (3.1)$$

and the central common corridor for $g_{KN\Sigma^2}$ calculated with h_0 and h_1 is

$$2.11 < g_{KN\Sigma^2} < 3.70 \quad (3.2)$$

which is compatible with the recent determinations of this constant using different sets of data.^{4,26,27}

Real parts of the $K^\pm n$ amplitudes have been calculated using this Stieltjes analysis. Figure 3 shows the transformed experimental points, D_n^- , corresponding to the fits of Table II, next to the allowed corridor for D_n^- obtained in this work, as well as the D_n^+ corridor. We obtain in particular rather different values for D_n^\pm at 10 GeV/c than the experimental ones^{8,12} but in agreement with the regeneration data at these energies, which give information on $|D_n^+ - D_n^-|$ (Refs. 26 and 28).

The $K^- n$ real parts obtained in this analysis are in general compatible with those calculated in Refs. 4 and 29 but somewhat lower in the 1.0–1.5 region, in such a way that our corridor slightly touches the Coulomb interference data⁵ (see Table III and Fig. 3). We have also obtained bounds on $D^\pm(0) = D^\mp(0)$ using our PA parametrization which are

$$-0.82 < D^\pm(0) < -0.56 \text{ fm}$$

and taking advantage of the fact that the PA are valid for a complex z , the position of the complex-conjugate zeros of $F^-(\omega)$, which plays an important role in logarithmic dispersion relations and as a stabilizer of the analytic continuation techniques,^{2,7,27,30} has been found to be

$$(0.35 \pm 0.05) \pm (0.16 \pm 0.04)i \text{ GeV/c} .$$

ACKNOWLEDGMENTS

I thank Dr. A. Cruz for many useful and stimulating discussions. I acknowledge the financial support of Comisi3n Asesora de Investigaci3n Científica y T3cnica (Plan Movilizador de la Físca de Altas Energías).

- ¹B. di Claudio, G. Violini, and N. M. Queen, Nucl. Phys. **B161**, 238 (1979).
- ²G. K. Atkin, J. E. Bowcock, and N. M. Queen, J. Phys. G **7**, 613 (1981).
- ³A. D. Martin, Phys. Lett. **65B**, 346 (1976).
- ⁴A. D. Martin, Nucl. Phys. **B179**, 33 (1981).
- ⁵P. Baillon *et al.*, Nucl. Phys. **B134**, 31 (1978).
- ⁶S. Ciulli, C. Pomponiu, and I. Sabba-Stefanescu, Phys. Rep. **17**, 133 (1975).
- ⁷J. Antolin and A. Cruz, J. Math. Phys. **27**, 104 (1986).
- ⁸J. Antolin, Zaragoza Report No. DFTUZ-86.2 (unpublished).
- ⁹N. M. Queen, University of Birmingham Report No. UB-Kp-1-78, 1978 (unpublished).
- ¹⁰V. Flaminio *et al.*, Report No. CERN-HERA 79-02, 1979 (unpublished).
- ¹¹J. Antolin and A. Cruz, J. Phys. G **12**, 297 (1986).
- ¹²P. Jenni *et al.*, Nucl. Phys. **B105**, 1 (1976).
- ¹³N. N. Nagels *et al.*, Nucl. Phys. **B147**, 479 (1976).
- ¹⁴O. Dumbrajs *et al.*, Nucl. Phys. **B216**, 277 (1983).
- ¹⁵V. Barger and R. J. N. Phillips, Nucl. Phys. **B32**, 93 (1971).
- ¹⁶R. Armenteros *et al.*, Nucl. Phys. **B21**, 15 (1970).
- ¹⁷M. Alston-Garnjost *et al.*, Phys. Rev. D **17**, 2266 (1978).
- ¹⁸A. J. Van Horn *et al.*, Phys. Rev. D **6**, 1275 (1972).
- ¹⁹M. Jones *et al.*, Nucl. Phys. **B90**, 349 (1975).
- ²⁰R. J. Hemingway *et al.*, Nucl. Phys. **B91**, 12 (1975).
- ²¹B. Conforto *et al.*, Nucl. Phys. **B105**, 189 (1976).
- ²²P. J. Litchfield *et al.*, Nucl. Phys. **B30**, 125 (1971).
- ²³T. H. Gronwall, Ann. Math. **33**, 101 (1932).
- ²⁴J. Gilewicz, *Approximats de Padé* (Lecture Notes in Mathematics, Vol. 667) (Springer, Berlin, 1978).
- ²⁵The whole data set, 120, minus the 11 discarded points by condition (i), minus the absorption point.
- ²⁶G. K. Atkin *et al.*, Phys. Lett. **95B**, 447 (1980).
- ²⁷J. Antolin, Z. Phys. C **31**, 417 (1986).
- ²⁸R. E. Hendrick *et al.*, Phys. Rev. D **11**, 536 (1975).
- ²⁹M. Alston Garnjost *et al.*, Phys. Rev. D **18**, 182 (1978).
- ³⁰G. K. Atkin *et al.*, Z. Phys. C **15**, 129 (1982).